Meniscus motion in a prewetted capillary

Andrei G. Egorov
Institute of Mathematics and Mechanics, Kazan State University, Universitetskaya 17, Kazan, Russia

Konstantin G. Kornev and Alexander V. Neimark
TRI/Princeton, 601 Prospect Avenue, Princeton, New Jersey 08542-0625

(Received 28 October 2002; accepted 8 July 2003; published 5 September 2003)

A conventional description of the effect of meniscus friction is based on the concept of the dynamic contact angle θ, which depends on the meniscus velocity V according to the Tanner law, $\theta \propto V^{1/3}$. However, recent high-resolution experiments on spontaneous uptake of wetting fluids by capillaries have questioned the universality of the Tanner law. We analyze a mechanism underlying the phenomenological concept of meniscus friction, which finds experimental confirmation. As a case study system, we consider a forced flow of meniscus in a cylindrical capillary. It is assumed that the capillary is prewetted and the coating uniform film could coexist with the static meniscus. Numerical analysis is restricted to van der Waals fluids for which the disjoining pressure Π as a function of film thickness h has the form $\Pi \propto h^{-3}$. For these fluids, the equilibrium apparent contact angle is zero. Within the lubrication approximation of the film flow, we show that the nonzeroth dynamic contact angle first appears when the fluid velocity exceeds a certain characteristic value. For smaller velocities, there is no appreciable distortion of the meniscus shape, compared to the equilibrium static configuration. The deformations of the film profile are concentrated at the transition zone between the macroscopic meniscus and the submicron precursor. While the concept of dynamic contact angle seems to be inappropriate for slow flows, the concept of contact line friction serves as a practical alternative to it. We show that when the velocity is slow and there is no visible contact angle, the friction is Newtonian, i.e., the relation between the pressure drop ΔP and the meniscus velocity is linear. As the velocity increases, the linear relation transforms into a nonlinear asymptotic law $\Delta P \propto (V \ln V)^{2/3}$. © *2003 American Institute of Physics.*
[DOI: 10.1063/1.1604392]

I. INTRODUCTION

There are a considerable number of papers aimed at explaining the phenomenon of dynamic contact angle (see, for review, Refs. 1–9). The approach is based on the classical hydrodynamic Bretherton model for propagation of a meniscus into a prewetted capillary.[10] This paper follows the same model with incorporation of disjoining pressure due to van der Waals forces. The film thickness ahead of the meniscus and the meniscus velocity are prescribed, and the aim is to predict the dynamic contact angle and pressure drop across the meniscus. The analysis is focused on the explanation of the abrupt appearance of the dynamic contact angle observed in the experiments.[11–16] In order to highlight the problem, we review the current state-of-the-art in the field of equilibrium and dynamic contact angles.[17]

A. Equilibrium meniscus and contact angle

When a capillary is partially filled with a wetting liquid, the latter forms a meniscus, which transits gradually into a uniform film coating the capillary wall. At static equilibrium, the film thickness h_∞ and the capillary radius R are interrelated due to the Derjaguin equation.[18,19] Indeed, the capillary pressure at the meniscus cupola $P_c = P_g - P_w$ is balanced at the uniform film by the Laplace pressure $\sigma/(R-h_\infty)$ (σ is the surface tension) and the disjoining pressure $\Pi(h_\infty)$:[19]

$$P_g - P_w = P_c = \left[\frac{\sigma}{R-h_\infty} + \Pi(h_\infty) \right]. \tag{1}$$

For wetting fluids we have $0 < \Pi(h) = \sigma\, a^{n-1}/h^n$, $a^{n-1} > 0$, $n > 1$; van der Waals films are typically characterized by $n=3$, $a \approx 1$ Å.[20]

If the meniscus is approximated by a semispherical cap of radius R_a, the radius of meniscus curvature is related to the current film thickness h and the inclination angle β as

$$R_a = \frac{h}{\cos\theta - \cos\beta} \tag{2}$$

(see Fig. 1 for definition of the contact angle).

Taking $h=R$, $\beta = \pi/2$, we come to the definition of apparent contact angle as $R_a \cos\theta = R$. Integrating the Laplace equation of capillarity augmented by disjoining pressure term, we have[21]

$$P_c = \frac{2\sigma\cos\theta}{R} = \frac{2\sigma}{R-h_\infty} + \frac{2}{(R-h_\infty)^2}\int_{h_\infty}^{R} (R-\xi)\Pi(\xi)\,d\xi. \tag{3}$$

Thus, at equilibrium, for the films with monotonous positive disjoining pressure isotherms, Eq. (3) gives formally a cosine theta greater than 1. Physically, the meniscus cupola is sus-

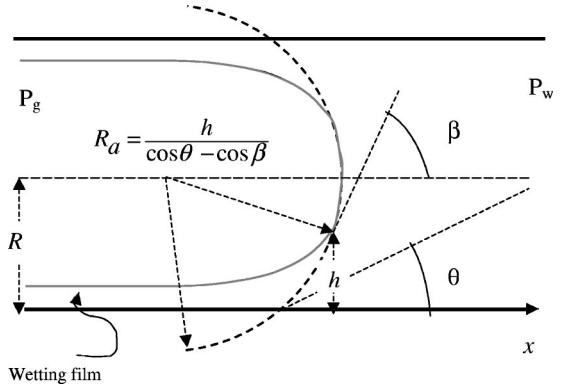

FIG. 1. The definition of apparent contact angle θ and geometric construction that helps to relate the meniscus radius and the apparent contact angle.

pended above the capillary wall and does not form any apparent contact angle.[22,23] Mathematically, to provide the transition from complete wetting to partial wetting, $\cos\theta<1$, the integral in (3) must be negative.

B. Moving meniscus

When a meniscus is forced to motion, the pressure in the film becomes different from the pressure at the meniscus cupola. Hence, Eq. (3) is not applicable anymore. At low velocities, the approximation of the meniscus shape as a spherical cap is still appropriate, but its radius R_m differs from the static value, R_e.[3,10] The macroscopic Bretherton theory that ignores the action of disjoining pressure in the precursor film seems to work well for wetting fluids at moderate velocities.[3,10] In accordance with Bretherton, an extra pressure due to viscous resistance scales as $\Delta P\propto(1/R_e-1/R_m)\propto(1-\cos\theta)\propto V^{2/3}$, thus giving the relation $\theta\propto V^{1/3}$, $\theta\ll 1$, known as the Tanner law.[24] The latter was confirmed experimentally for moderate meniscus velocities.[3,10] On the other hand, there is a series of experiments in which the apparent radius of the meniscus and consequently the *dynamic contact angle* change abruptly as the velocity attains a critical value, typically, $V_{cr}\sim 10^{-3}$ cm/s.[11–16] Therewith, even without a visible change of the wetting conditions keeping the contact angle unchanged, menisci manifest an enhanced resistance.[25]

The existing theories can neither capture the effect of abrupt formation of the dynamic contact angle nor explain the observed dependency of the friction force on the meniscus velocity at low speeds (see, for review, Refs. 1–9). In the attempts to extend the Bretherton theory to account for the flow in a precursor submicron film, the main attention was paid to the regime of moderate velocities.[4,5,26] In particular, a detailed work of Kalliadasis and Chang[26] addresses an asymptotic limit of weak adhesion when viscous forces are dominating. As was expected, in this limit the Tanner law works and the prefactor is a universal constant independent of the thickness of precursor film and adhesion properties of liquid/substrate pair.

C. Objectives and paper outline

We consider the problem of meniscus motion focusing on the low velocity regime. We restrict our analysis to simple wetting van der Waals' liquids. The absorption layer forming the precursor film ahead of the meniscus is postulated to be the *equilibrium* one. In this respect, the spreading is controlled by the adhesion forces, in contrast to the case of thick films, where it is controlled by the viscous forces.[17,26] The equilibrium film thickness can be eliminated from the input parameters by using Eq. (1). Therewith, two length scales, the radius of capillary R and the van der Waals parameter a, characterize the property of the given fluid/capillary pair.

Intuition based on the experience with the Bretherton model does not turn out true when the adhesion forces play a dominant role. In particular, the hydrodynamic bending of the film profile does not lead to an immediate appearance of the dynamic contact angle just after a meniscus starts to motion. We show that the concept of dynamic contact angle is applicable only for a range of advancing velocity (or specific range of capillary radii) exceeding a certain critical value: at low velocities, the meniscus slides over the precursor film being suspended above it as it would be in statics. The contact angle first appears at some critical velocity V_{cr}. For van der Waals fluids with $n=3$, this critical velocity is expressed as $V_{cr}=|U_{cr}|(\sigma/3\eta)(h_\infty/a)^{-3}$, $U_{cr}=-1.79$. That is, the theory explains the experimental observations of an abrupt appearance of the dynamic contact angle.

We also explore the origin of the friction force term F_{fr}, phenomenologically describing the effect of contact line friction in the generalized Lucas–Washburn equation modeling the capillary rise dynamics:[25,27,28]

$$8\eta x\,dx/dt+F_{\mathrm{fr}}=2R\sigma-\rho R^2 g x. \tag{4}$$

In this equation, the first term is caused by the Poiseuillean friction of the fluid column of length x, and F_{fr} is the friction force caused by the contact line resistance and expressed by Eqs. (30) and (32). On the right side is the difference between capillary force pulling the meniscus upward and the gravitational force opposing the meniscus advance. ρ is the fluid density, and η is the viscosity. As shown in Ref. 25, the experiments can be interpreted in terms of Eq. (4) with Newtonian friction, $F_{\mathrm{fr}}\propto dx/dt$. Our analysis confirms these findings. In particular, a cofactor is obtained as a function of adhesion properties of the film/substrate pair. As the velocity increases, the linear relation is transformed into a nonlinear one with a logarithmic behavior as $|V|\to\infty$ (that is in agreement with Ref. 29).

The paper is organized as follows. In Sec. II we formulate the problem in the lubrication approximation. The boundary conditions are discussed in detail to show how to extract the apparent contact angle and extra pressure from the given film profile. In Sec. III we perform an asymptotic analysis of the problem. Two types of solutions, which correspond to droplets and menisci, are found. We specify the meniscus solutions by constructing a proper algorithm for a numeric selection of the needed solution from the family of solutions. In Sec. IV we analyze the results and compare the

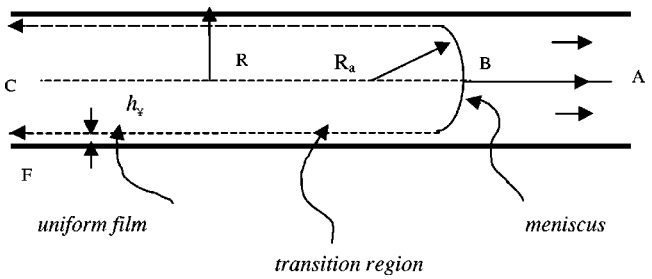

FIG. 2. Fixed reference frame, $s=x-Vt$, velocity V is negative: *advancing meniscus*. Capillary moves from left to right. The meniscus, as a balloon, is kept motionless by applying a force F (which corresponds to the tensile "wetting force").

theoretical predictions with available experimental data. Section V summarizes the results.

II. PROBLEM FORMULATION

Because of the problem's complexity, some reasonable simplifications have been proposed in the literature.[1–9] Considering the problem of dynamic wetting, the major attention was paid to the transition zone between the uniform precursor film and the meniscus. In particular, following the seminal works by Landau and Levich[30] and Derjaguin,[31] the lubrication approximation is invoked to describe the profile of thin films, assuming $h_\infty \ll R$. We also follow this approach and assume that the thickness of the precursor film far ahead of the meniscus equals the *equilibrium film thickness* h_∞. The discussion of this hypothesis can be found elsewhere.[9,32]

A. Transition zone in the Landau–Levich–Derjaguin model

The flow can be subdivided into three regions: uniform film at the left, semispherical meniscus at the right, and transition zone in the middle (Fig. 2). We use the traditional scheme of lubrication theory, the so-called Landau–Levich–Derjaguin (LLD) model.[30,31] The model is restricted to regimes of small Reynolds numbers, $\mathrm{Re}=\rho|V|R/\eta \ll 1$. The velocity profile is the Poiseuillean parabolic; the small slope approximation allows us to assume the pressure uniformity across the film. Also, it is presupposed that the inequality $(h_\infty/R)^2 \ll (\eta|V|/\sigma)^{2/3}$ holds. This condition makes it possible to neglect the disjoining effect of viscous flow, which, due to nonequidistant streamlines, contributes to disjoining pressure a term proportional to the film thickness.[33]

The pressure in the wetting film differs from the constant pressure in the gas, and the difference is just the capillary pressure jump plus disjoining pressure. Assuming that the gas viscosity is zero, the volumetric flow rate is written as[30,31]

$$q=-\frac{h^3}{3\eta}\frac{\partial P_w}{\partial x}. \tag{5}$$

Here, η is the viscosity of wetting fluid, h is the wetting film thickness, and x is the spatial coordinate measured along the capillary. In order to take into account the adhesion forces, the pressure is written in accordance with the Derjaguin formula as[31]

$$P_w=P_g-2\sigma H-\Pi(h). \tag{6}$$

Here, $2H\approx \partial^2 h/\partial x^2+1/R$ is the curvature of the interface. The mass balance equation,

$$\frac{\partial h}{\partial t}+\frac{\partial q}{\partial x}=0, \tag{7}$$

completes the model. Traveling wave solutions to the model (5)–(7) are our interest.

B. Traveling wave solutions

For these solutions, the problem (5)–(7) is reformulated in the fixed reference frame, $s=x-Vt$, where the negative parameter V denotes the *given* velocity of advancing meniscus.

In the moving frame, Eq. (7) can be integrated once to decrease the order from fourth to third. After integration it takes the familiar Landau–Levich–Derjaguin form as

$$-\frac{3\eta V}{h^3}(h-h_\infty)=\frac{d}{ds}P_w(h) \tag{8}$$

or

$$\frac{3\eta V}{\sigma h^3}(h-h_\infty)=\frac{d}{ds}\left(\frac{d^2h}{ds^2}+\frac{a^{n-1}}{h^n}\right). \tag{9}$$

Thus, two physical parameters enter the model: the equilibrium film thickness h_∞ and the meniscus velocity V. Restricting ourselves to a similarity solution, we focus on derivation of a relation between meniscus velocity and appropriate pressure drop for given h_∞. Therewith, an analysis of the meniscus shape, precisely its apparent radius as a function of the meniscus velocity, must be performed by taking V and h_∞ as *independent* parameters of the model. The independence of V from h_∞ makes the problem different from the traditional Bretherton formulation.[10]

C. Boundary conditions

Equation (9) is subject to three boundary conditions. A couple are formulated at the left infinity, and one at the right infinity, where the film merges into the meniscus. At the left infinity, due to our assumption, the film is uniform and its thickness equals the equilibrium film thickness h_∞ [h_∞ is the solution of Eq. (1)]

$$h=h_\infty, \quad \text{as} \quad s\to-\infty. \tag{10}$$

The meniscus apparent radius is unknown in advance. This makes the formulation of the boundary condition at the right infinity challenging. In order to find this condition, we use the geometrical construction depicted in Fig. 1. The chain of relations

$$h=R-R_a\cos\beta, \quad \text{and} \quad \cos\beta\approx 1-\frac{1}{2}\left(\frac{dh}{ds}\right)^2,$$

results in the formula

$$2\frac{R_a-R}{R_a}\approx\left(\frac{dh}{ds}\right)^2-2\frac{h}{R_a}=\left(\frac{dh}{ds}\right)^2-2h\frac{d^2h}{ds^2},$$

which finally gives the boundary condition as

$$R\frac{d^2h}{ds^2}=1-F(V)\quad \text{as}\ \ s\to\infty, \tag{11}$$

where F denotes the following:

$$F(V)=\lim_{s\to\infty}\left[\frac{1}{2}\left(\frac{dh}{ds}\right)^2-h\frac{d^2h}{ds^2}\right]. \tag{12}$$

Due to our hypothesis, the thickness of the precursor film corresponds to its equilibrium value. Therefore, the radius of capillary in Eq. (11) can be expressed through this thickness. Writing Eq. (11) for static meniscus, we have

$$R\frac{d^2h}{ds^2}\bigg|_{V=0}=\frac{R}{R_e}=1-F(0).$$

On the other hand, expressing the radius of equilibrium meniscus R_e and the function $F(0)$ by using the results of Appendix B, we have

$$R_e=\frac{h_\infty^n}{a^{n-1}},\quad F(0)=-\frac{3}{2}\left(\frac{a}{h_\infty}\right)^{n-1}.$$

Substituting these values into Eqs. (11) and (12), we rewrite the boundary condition in the form

$$R_e\frac{d^2h}{ds^2}=\frac{1-F(V)}{1-F(0)}\ \ \text{as}\ \ s\to\infty, \tag{13}$$

which does not contain the radius of capillary.

D. Dimension analysis

Introducing the dimensionless variables as

$$z=h/h_\infty,\quad X=s/L,\quad L=h_\infty/\sqrt{\varepsilon},\quad \varepsilon=(a/h_\infty)^{(n-1)},$$

where L is the characteristic length scale, associated with the molecular scale a, Eq. (9) is rewritten as

$$\frac{U}{z^3}(z-1)=\frac{d}{dX}\left(\frac{d^2z}{dX^2}+\frac{1}{z^n}\right). \tag{14}$$

Here, $U=-\mathrm{Ca}\,\varepsilon^{-3/2}=-3|V|\eta\varepsilon^{-3/2}/\sigma$ is the product of the capillary number Ca and the adhesion factor ε. Solutions to the full problem depend only on the parameter U. A remarkable property of Eq. (14) is its scaling invariance with respect to the change of variable, $\hat{X}=|U|^{1/3}X$.[34] In the new variable, Eq. (14) reads

$$-\frac{1}{z^3}(z-1)=\frac{d}{d\hat{X}}\left(\frac{d^2z}{d\hat{X}^2}+\frac{|U|^{-2/3}}{z^n}\right). \tag{15}$$

The latter shows that in the asymptotic limit as $|a|\to 0$ we arrive at the Bretherton case.[10]

In dimensionless variables the boundary conditions take the form

$$z=1,\ dz/dX=0\ \ \text{as}\ \ x\to-\infty, \tag{16}$$

$$\frac{d^2z}{dX^2}=\frac{1-\varepsilon F(U)}{1-\varepsilon F(0)}\quad \text{as}\ \ X\to\infty, \tag{17}$$

where the function F remains invariant under the change of variables

$$F(U)=\lim_{X\to\infty}\left[\frac{1}{2}\left(\frac{dz}{dX}\right)^2-z\frac{d^2z}{dX^2}\right],\quad F(0)=-3/2.$$

As a rule, the parameter ε is very small, so that we seek the solution in the form

$$z=z_0+\varepsilon z_1+\cdots. \tag{18}$$

Restricting ourselves to the leading order term, we rewrite Eq. (17) as

$$\frac{d^2z_0}{dX^2}=1,\quad \text{as}\ \ X\to\infty. \tag{19}$$

As we will show below, the approximation (19) is valid only for finite U. When U tends to infinity, $F(U)$ increases accordingly, and the scheme of regular perturbations (18) does not work anymore.

E. Pressure drop and contact angle

When the meniscus moves through a capillary, the "dynamic pressure drop," which is caused by the viscous forces, augments the Laplace pressure drop. Therefore, an excess pressure drop, i.e., the pressure drop additional to the equilibrium capillary pressure, is the characteristic parameter of the motion. It can be calculated by integrating Eq. (9) as

$$\Delta P=\frac{2\sigma}{R_a}-\frac{2\sigma}{R_e}=\int_{-\infty}^{\infty}\frac{3\eta V}{h^3}(h-h_\infty)ds. \tag{20}$$

Written in dimensionless form, this equation gives the relation between the pressure drop normalized by σ/R and U as

$$\frac{\Delta PR}{\sigma}=\varepsilon(F(U)-F(0))\big|_{\varepsilon=0}+O(\varepsilon^2)$$

$$=|U|\int_{-\infty}^{\infty}\frac{z-1}{z^3}dX. \tag{21}$$

The contact angle can be expressed in terms of the derivatives of the film profile using the small slope approximation. The same geometrical construction as above with the definition $\cos\theta=R/R_a$ gives us the definition of the contact angle via the derivatives of the film profile at the right infinity. In the limit $\theta\sim o(1),\beta\sim o(1)$, the contact angle behaves asymptotically as

$$\theta=\sqrt{\varepsilon F(U)}. \tag{22}$$

This formula shows that a possibility of introduction of a contact angle is associated with the change of the sign of $F(U)$ from negative in static case to positive in dynamic case.

III. ANALYSIS

Before proceeding to an investigation of the boundary value problem Eqs. (14), (16), and (19), let us perform a

local analysis of the solutions to Eq. (14) for two limiting cases: $z_0 \to \infty$ and $z_0 \to 1$. This analysis will help us to construct an algorithm for solving the boundary value problem, (14), (16), and (19).

A. Asymptotic analysis of solutions at the meniscus cupola: Simplification of the LLD equation

At the meniscus cupola, it is more convenient to use Eq. (15) instead of Eq. (14). We restrict ourselves to the disjoining pressure isotherms with the characteristic exponent $n > 1$. Assuming monotonicity of the film profile as $z_0 \to \infty$, the order of Eq. (15) can be reduced to the second by using a new variable $y = y(z_0)$ defined as $dz_0/d\hat{X} = \sqrt{y(z_0)}$. Equation (15) is rewritten as

$$-\frac{2}{\sqrt{y}}\frac{z_0-1}{z_0^3} = \frac{d}{dz_0}\left(\frac{dy}{dz_0} + \frac{2|U|^{-2/3}}{z_0^n}\right). \tag{23}$$

Introducing another variable as

$$z_0 = e^p,$$

we arrive at the equation

$$-\frac{2}{\sqrt{y}}(1-e^{-p}) = \frac{d^2y}{dp^2} - \frac{dy}{dp} - 2n|U|^{-2/3}e^{-(n-1)p}. \tag{24}$$

For $n > 1$, this equation has quite universal behavior as the variable t tends to infinity. Indeed, neglecting exponentially small terms, we get the equation

$$-\frac{2}{\sqrt{y}} = \frac{d^2y}{dp^2} - \frac{dy}{dp}. \tag{25}$$

The latter has the explicit solutions expressed via the Airy functions.[35] Duffy and Wilson[36] have done a detailed analysis of the explicit solutions of Eq. (25). In particular, they found two classes of solutions. The solutions are distinguished by different asymptotic behavior at infinity. Instead of utilizing the explicit (yet quite complicated) expressions, we study the phase portrait of Eq. (25). This investigation enriches the Duffy–Wilson approach and allows us to specify the family of solutions appropriate for our particular problem.

B. Phase portrait: Moving droplets and menisci as two types of traveling wave solutions

Written as the dynamic system

$$x_1 = 2^{-2/3}y, \quad x_2 = 2^{-2/3}dy/dp,$$

Eq. (25) takes the form

$$\dot{x}_1 = x_2, \quad \dot{x}_2 = x_2 - 1/\sqrt{x_1}. \tag{26}$$

Here, dots denote differentiation with respect to p. One can imagine a flow of a fictitious fluid with velocity components (x_1, x_2). The flow takes place in the right semiplane $x_1 > 0$. In Appendix A we present detailed calculations that lead to the phase portrait depicted in Fig. 3. We can interpret the solutions by taking into account their specific behavior as $z \to \infty$.

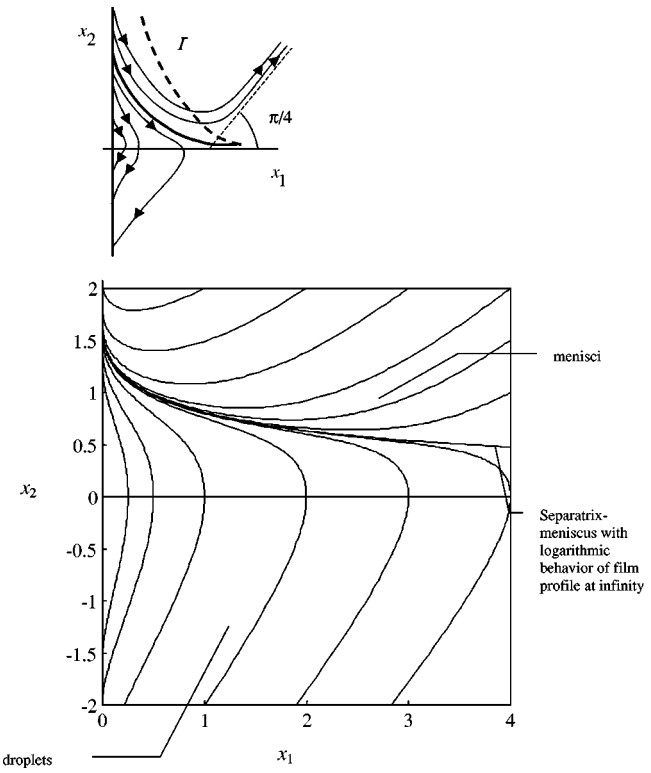

FIG. 3. Phase plane of system (26). (a) Schematic of the phase portrait with characteristic lines. The bold curves are separatrices; Γ is the line of turnover points. The dashed straight line is the asymptote of U-shaped trajectories. (b) Phase portrait obtained numerically.

Droplets and menisci

Since we are looking for solutions describing menisci transiting to spherical cupolas, the following asymptotic behavior is expected for these solutions:

$$z_0 \propto \hat{X}^2, \quad dz_0/d\hat{X} \propto \hat{X} \propto \sqrt{z_0},$$

$$y = (dz_0/d\hat{X})^2 \propto z_0, \quad dy/dp \propto z_0.$$

Therefore, the trajectories corresponding to menisci must have the asymptotic behavior $x_2 \propto x_1$ at infinity. Consequently, the V-shaped trajectories describe menisci. Below the separatrix, starting from the point $x_2 = A^*$, $x_1 = 0$, the trajectories never grow like $x_2 \propto x_1$. Numeric integration of system (26) gives $A^* = 1.617$. The separatrix solution corresponds to the Hervet–de Gennes solution[37] (see also the discussion of solution stability in Refs. 9, 34). The characteristic feature of the trajectories situated below the separatrix is the opposite sign of curvature of the corresponding film profile. Matched with the precursor films, these solutions describe droplets.

C. Asymptotic analysis of solutions in the vicinity of uniform film

Linearization of Eq. (14) about the equilibrium film thickness (see, for example, a similar analysis done in Refs. 4, 5) shows that the asymptotic solutions take the forms

If $U<U<-2n\sqrt{n/3}/3$:

$$z_0-1=C\exp(kX)\sin(\upsilon X-\alpha),\quad 0\leqslant\alpha<2\pi, \tag{27}$$

If $0>U>-2n\sqrt{n/3}/3$:

$$z_0-1=C(\exp(k_1X)\sin(\alpha)+\exp(k_2X)\cos(\alpha)),$$
$$0\leqslant\alpha<2\pi.$$

The parameters k,υ,k_1,k_2 are associated with the roots of the cubic equation

$$Z_0^3=nZ_0+U. \tag{28}$$

The roots must have a positive real part. In the first line of Eq. (27), the parameters k and υ correspond to real and imaginary parts of the roots $Z_0=k\pm i\upsilon$. In the second line, k_1 is k_2 are positive roots of Eq. (28). Due to a translational symmetry, we can set $C=1$ in both lines of Eq. (27). Thus, while solving the problem (14), (16), and (19) by the shooting method, we use the parameter α to meet with the boundary condition at the right infinity.

IV. RESULTS

A. Numeric analysis of the LLD model

The zeroth approximation imposes a constraint, namely, integration of Eq. (14) with the boundary condition (19) shows that the equality

$$\int_{-\infty}^{\infty}\frac{z_0-1}{z_0}dX=0$$

holds. Thus, the film profile should have at least one indentation with the thickness at the cavern smaller than the equilibrium film thickness. In calculations, we restricted ourselves to the Hamaker–Lifshitz approximation for disjoining pressure, $n=3$. Therewith, the thickness of the precursor film is $h_\infty=(a^2R)^{1/3}$. In Fig. 4, we plot the characteristic shapes of the transition zone depending on the meniscus velocity. The amplitude of the waves ahead of the meniscus goes to zero very fast and at infinity, the waves form almost invisible tiny ripples. The existence of indentations or ripples is necessary for getting the nonzeroth apparent contact angle. As mentioned above, the apparent contact angle expressed through the function F, Eq. (22), is the complex valued function of U. A numeric analysis reveals that the function F is negative at $|U|<|U_{cr}|=-1.79$. Therefore, the contact angle cannot be introduced if $|U|<|U_{cr}|$. For $|U|>|U_{cr}|$, the function F is positive. Figure 5 shows the dependence of the apparent contact angle on the meniscus velocity.

Remarkably, the pressure drop needed to keep the meniscus moving is well defined within the whole range of velocities. Within our perturbation scheme, the pressure drop, which is of ε order, can be calculated by using the leading order approximation and the left-hand side of Eq. (21). When the meniscus velocity is small, the calculations similar to those presented in Ref. 38 (see Appendix B) show that the pressure drop is a linear function of the meniscus velocity. In this range of U, the meniscus shape is almost unperturbed compared to its equilibrium profile. When the velocity increases, the transition zone cannot be maintained in a quasiequilibrium anymore. The viscous forces contribute to the stress at the film surface, thus making the surface significantly folded. As a result, the relations between the

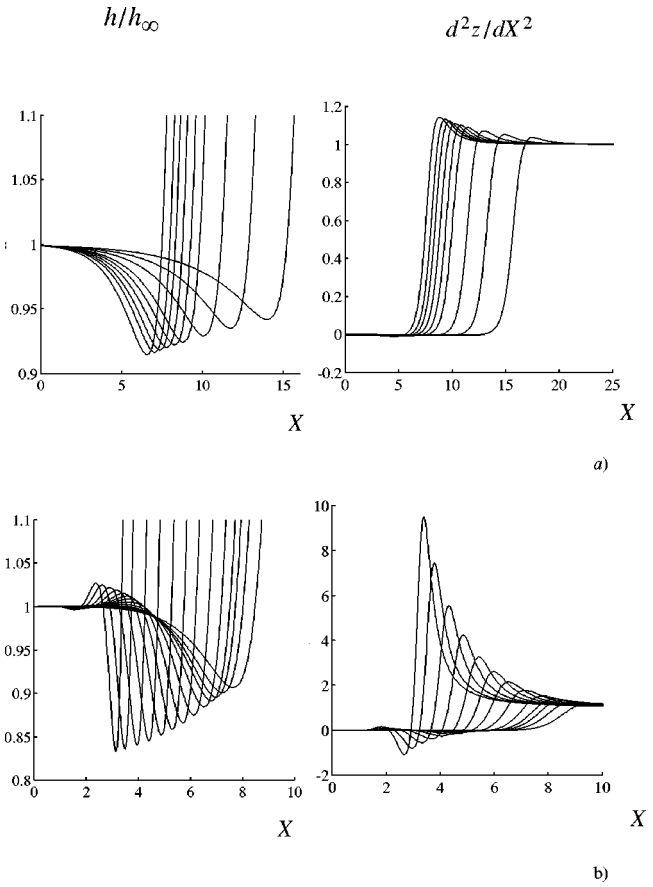

FIG. 4. Characteristic pattern of the moving films in transition zone. Left column is film height as a function of coordinate; right column is dimensionless curvature as a function of coordinate. (a) From the right to the left: $U=-0.9,-1.1,-1.3,-1.5,-1.6,-1.7,-1.8,-1.9,-2$. (b) From the right to the left: $U=-2.5,-3,-3.5,-4,-5,-7,-10,-14,-20,-30,-45,-70,-100$.

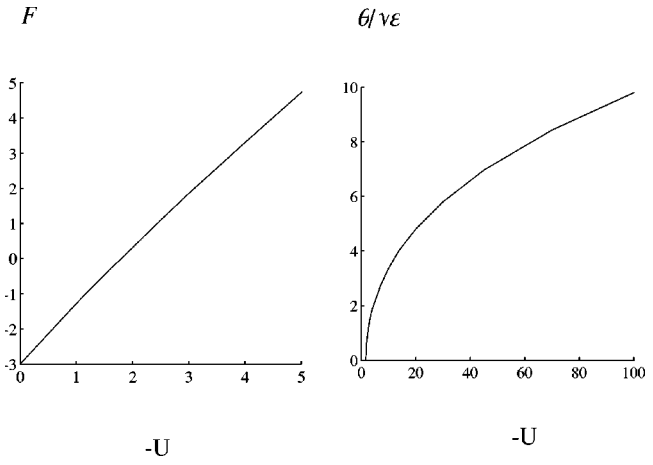

FIG. 5. In asymptotic limit as $U\to 0$ the function F is negative, $F(0)=-3$. The contact angle occurs only for $|U|>1.79$.

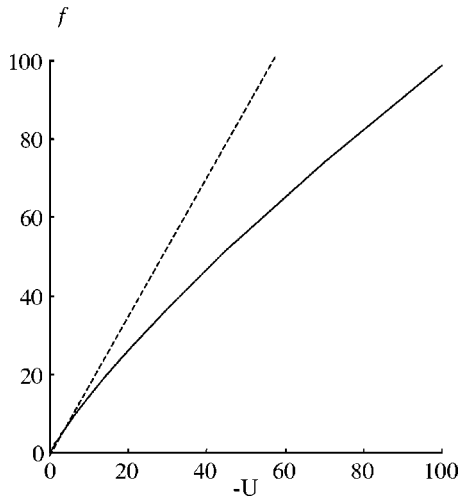

FIG. 6. The function $f(U)$. The pressure drop normalized by σ/R varies linearly as $U\to 0$, quasistatic regime of displacement.

pressure drop, apparent contact angle, and meniscus velocity become nonlinear. The dimensionless pressure drop is given by

$$\frac{\Delta P R}{\sigma}=\left(\frac{a}{R}\right)^{2/3}(-3+f(U)), \tag{29}$$

with the function f depicted in Fig. 6. Approximating the numeric data as

$$f(U)=A(U\ln(1+B\sqrt{-U}))^{2/3}, \tag{30}$$

we get for parameters A and B the values $A=2.957$, $B=0.475$. Equation (30) gives us a correct asymptotic behavior of the solution at low and high velocities.

As already noted, for $U_{cr}>-1.79$, the meniscus shape remains almost unchanged with no apparent contact angle. Thus, the contact angle concept fails in this range of U. But, this concept is not necessarily the only way to explain the experimental data. Instead, it is better to consider a velocity-dependent friction force, which is well defined in the whole range of velocities. Below, we show how this concept works.

B. Application of the friction force concept to the Lucas–Washburn equation

It is instructive to numerically estimate the range of velocities at which an apparent contact angle first appears. Consider *hexadecane* as a typical van der Waals fluid. The Hamaker–Lifshitz approximation with $n=3$ and $a\approx 1$ Å is appropriate here. Upon substitution of the physico-chemical parameters for hexadecane into the inequality

$$|V|>V_{cr}=|U_{cr}|\frac{\sigma}{3\eta}(h_\infty/a)^{-3}, \tag{31}$$

we come up with the following estimates:

$h_\infty/a=10$, $R=100$ nm$=0.1$ μm,

$|V|>1.79\cdot 10^{-3}\cdot 273\approx 0.5$ cm/s,

$h_\infty/a=100$, $R=10$ μm,

$|V|>1.79\cdot 10^{-6}\cdot 273\approx 5\cdot 10^{-4}$ cm/s.

In the vicinity of U_{cr}, the relation between the pressure drop and meniscus velocity is almost linear (Fig. 6). Thus, in applications to flows of oils in underground reservoirs, we deal, most likely, with the Newtonian regimes of meniscus friction. In general, in order to interpret the experimental data, it is more practical to use the nonlinear relations (29)–(30). Introducing the friction force $F_{\rm fr}$ applied to the wetting perimeter, we can rewrite the generalized Lucas–Washburn equation for the capillary rise in the form of Eq. (4) with

$$F_{\rm fr}=\sigma R\left(\frac{a}{R}\right)^{2/3}(-3+f(U)),\quad U=\frac{-R\eta}{a\sigma}\frac{dx}{dt}. \tag{32}$$

The function $f(U)$ is defined by Eq. (30) and depicted in Fig. 6. In particular, for the quasistatic regime of meniscus advance, when the linear relation $f\propto U$ holds, Eq. (4) is identical to that used in Ref. 25 for interpretation of experimental data. A linear dependence of the friction force caused by the contact line friction has been suggested phenomenologically in Refs. 25, 39–43. In Refs. 8 and 38, the linear friction of the contact line has been justified for a particular problem of friction of a foam lamella. As shown in recent experiments,[25] the generalized Lucas–Washburn equation (4) is capable of describing experimental observations if one uses for the friction force the formula $F_{\rm fr}=2\chi R\,dx/dt$, where the friction coefficients for ethanol is $\chi\approx 0.04$ Pa·s, and is $\chi\approx 0.45$ Pa·s for water.

It is interesting to compare the model with a constant friction coefficient and the model with a velocity-dependent friction coefficient. The adhesion properties of water cannot be described by a simple monotonous disjoining pressure isotherm.[19] Hence, an interpretation of the data for water is beyond the scope of this paper. On the other side, ethanol is a typical van der Waals fluid and we can use Eq. (32). The molecular parameter a is an adjustable parameter of the model. Taking the following experimental data:

$\eta=1.17$ mPa·s, $R=0.295\cdot 10^{-3}$ m,

$\sigma=2.2\cdot 10^{-2}$ N/m,

as the input parameters, the solutions of Eqs. (4) and (32), subjected to the initial condition $x(0)=0$, can be fitted into the experimental data. Selecting $a=3\cdot 10^{-10}$ m, we calculate the equilibrium thickness as $h_\infty=0.019\cdot 10^{-3}$ m. With these parameters, we describe the data perfectly (Fig. 7). As seen from the picture, the experimental data can be explained by either linear Newtonian friction with the coefficient $\chi\approx 0.04$ Pa·s found experimentally or by non-Newtonian friction with the theoretical parameters taken from Eqs. (30) and (32). This favors the consideration of the precursor film as the equilibrium absorption film. In other applications, for example, when the meniscus slides over a nonequilibrium film, the function $F_{\rm fr}=F_{\rm fr}(U)$ must be specified for each particular h_∞. This problem is beyond this paper's scope.

V. CONCLUSIONS

Employing the Landau–Levich–Derjaguin model, we studied the drag mechanism of a meniscus moving in a cy-

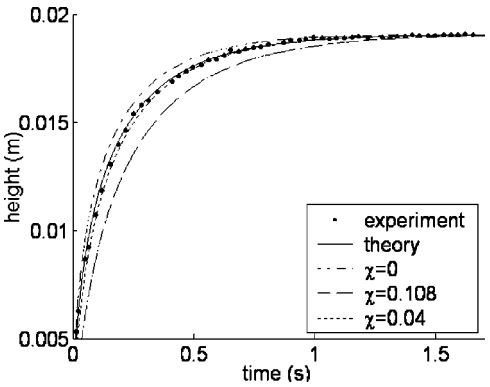

FIG. 7. Experimental and theoretical analyses of the capillary rise dynamics. The linear Newtonian friction law with the coefficient $\chi \approx 0.108$ calculated from Eq. (30) as $U \to 0$ is unable to explain the data in this range of velocities.

lindrical capillary. The objects of the study were van der Waals' liquids, which wet capillaries completely. The model describes the film profile of the transition zone between the uniform precursor film ahead of the meniscus and the meniscus cupola. The thickness of the precursor film is assumed to be equilibrium, so that a static meniscus would coexist with such a film. The main attention is paid to the explanation of experimental observations that the dynamic contact angles appear abruptly as the meniscus velocity overcomes a certain value.[11–16] Because the critical velocity of the appearance of dynamic contact angles is very small, the model is restricted to small Reynolds and capillary numbers.

We derived a new boundary condition to the LLD equation in the form of Eqs. (11), (12), and (13), which links the curvature of meniscus cupola with the lower derivatives of the film profile. When the adhesion forces prevail over the viscous ones, the boundary condition implies that the meniscus curvature is almost equilibrium with a correction term of the order of $(a/h_\infty)^{n-1}$, where a is the molecular parameter of the disjoining pressure isotherm, n is the exponent of the disjoining pressure isotherm, and h_∞ is the thickness of precursor film. Thus, the boundary condition in its leading order is analogous to the Bretherton condition to the Landau–Levich equation when there are no adhesion forces. A straightforward numeric approach to the problem is complicated by the fact that the LLD equation has two classes of solutions describing droplets and menisci. Extending the Duffy–Wilson analysis[36] by investigating the phase portrait of the LLD equation, we specified the location of menisci. Selecting an appropriate family of solutions, we studied the problem numerically by the shooting method.

It is shown that the LLD equation explains the abrupt appearance of the dynamic contact angle. At low velocities, the meniscus is suspended above the precursor film, so that the macroscopic contact angle is zero. At some velocity, when the hydrodynamic bending of the precursor film becomes perceptible, the macroscopic meniscus first touches the capillary walls. The dynamic contact angle could be introduced as a parameter bearing a physical meaning only for larger velocity. Mathematically, the contact angle is a complex valued function, which is imaginary at low velocities and real only when the velocity overcomes a certain barrier defined by Eq. (31). Compared to the dynamic contact angle, an extra pressure needed to keep the meniscus moving is a well-defined physical quantity. It varies linearly at low velocities, thus demonstrating the applicability of the Newton law of friction to describe the resistance of the contact line. As velocity increases, the Newtonian approximation no longer works, and a numeric analysis suggests the approximate formula (30). The latter has correct asymptotes at low and "high" velocities, $3|V|\eta(h_\infty/a/)^{3(n-1)/2}/\sigma \gg 1$. It should be noted that the model must be modified at high velocities, because our employed perturbation scheme does not work in that region.

We applied the developed theory to an analysis of experimental data on capillary rise dynamics.[25] Generalizing the Lucas–Washburn equation by including the contact line friction, Eqs. (4) and (32), we showed that the experiments can be explained satisfactorily. An extension of the approach to polar fluids such as water seems promising. In particular, a justification of the Newtonian friction of the contact line can be done immediately in a way outlined in Appendix B. However, due to a nonmonotonicity of the disjoining pressure isotherms, the behavior of the dynamic contact angle for polar fluids is much more complex as compared to the van der Waals' case.

ACKNOWLEDGMENTS

The work is supported by the Johnson & Johnson Focused Giving Program and a group of TRI/Princeton corporate members.

APPENDIX A: AN ANALYSIS OF PHASE PORTRAIT

Singularities

The points $(0,\infty)$, (0,0), both coordinate lines, and a family of points situated at the line $x_2 = 1/\sqrt{x_1}$ are singular for system (26).

We first investigate the behavior of the system near the x_2 axis. Consider the one-parametric ansatz $x_2 = A + \varepsilon(x_1)$, $|\varepsilon(x_1)| \ll 1$, $x_1 \ll 1$ with a constant A. Substituting this ansatz into Eq. (26), we get the asymptotic solution $x_2 = A - 2\sqrt{x_1}/A + (1 - 2/A^3)x_1 + o(x_1\sqrt{x_1})$. The derivative dx_2/dx_1 tends to infinity; hence, any trajectory of system (26) starts from/ends at the x_2 axis *tangentially*. For positive A, the derivative is negative at the x_2 axis, while for negative A, this derivative is positive.

The x_1 component of the vector field changes sign at the x_1 axis: in the upper quadrant, this component is positive, and it is negative in the lower quadrant. The derivative dx_2/dx_1 tends to infinity as the trajectory approaches the x_1 axis. Therefore, the x_1 axis is a set of turnover points.

The point (0,0) deserves special attention, because it gives birth to a special flow pattern. Using the characteristic features of the trajectories, we conclude that near this point, the trajectories are quasicyclic. Starting from the x_2 axis in the upper quadrant, they pass through a turnover point at the x_1 axis and come back to the negative x_2 axis, thus avoiding the point (0,0) from the right. We term these trajectories

''quasi'' because they are not closed, yet can be imagined as fragments of cycles. Therefore, the vector field near the origin of coordinate can be imagined as that produced by a vortex. The continuation principle tells us that there is a finite flow domain possessing similar vortex flow pattern. The specificity of such a pattern is that the x_2 component of this field does not change the sign.

However, the sign definiteness of the x_2 component cannot be prescribed for the whole phase plane. Inspection of the second equation of system (26) shows that the x_2 component might change the sign whenever a trajectory crosses the line $x_2=1/\sqrt{x_1}$. This line contains a set of turnover points; below the line $x_2=1/\sqrt{x_1}$, the trajectories are descending curves, while they are ascending above it. As x_1 tends to infinity the trajectories behave as $x_2 \propto x_1$. Summarizing the above analysis, we come to the conclusion that above a certain positive $A=A^*$, the trajectories take the U-like form. Therefore, there exists a boundary, *separatrix*, selecting the quasicyclic trajectories from the U-like ones.

This separatrix must lie below the curve of turning points for V-shaped trajectories, $x_2=1/\sqrt{x_1}$, but higher than the x_1 axis. To specify the separatrix, we consider its behavior at infinity, $x_1 \to \infty$, where the separatrix branches from the x_1 axis. Consider the new variable $x_1=Y^{-2}$. This change of variable maps infinity to zero. In vicinity of the point $Y=0$, the integral curves are described by the following equation:

$$-\frac{Y^3}{2}\frac{dx_2}{dY}=1-\frac{Y}{x_2}. \tag{A1}$$

The direct calculations show that the one-parametric ansatz $x_2=B+\varepsilon(Y)$, $|\varepsilon(Y)| \ll 1$ does not satisfy Eq. (A1), provided that x_2 is negative. This tells us that no trajectories with a nonzeroth x_2 occur as $Y \to 0$. Choosing the following form $x_2=aY^{\mu}$, we get two possibilities: either (i) $a=1$, $\mu=-2$, or (ii) $a=1$, $\mu=1$. The former results in the asymptotic behavior $x_2 \propto x_1$ for U-shaped trajectories, negative x_2 being inadmissible. The latter with $\mu=1$ is suitable for the description of separatrix with the asymptotic behavior $x_2 \propto 1/\sqrt{x_1}$. However, we see that both signs, plus and minus, are admissible for Y. Considering the next terms in asymptotic expansion as $x_2=Y(1+\varepsilon)$, $|\varepsilon(Y)| \ll 1$, we arrive at the equation

$$\frac{Y^4}{2}\frac{d\varepsilon}{dY}+\left(\frac{Y^3}{2}+1\right)\varepsilon-\varepsilon^2+\varepsilon^3+\frac{Y^3}{2}=0. \tag{A2}$$

This equation has the asymptotic solution

$$\varepsilon=-\frac{Y^3}{2}\left(1-\frac{5Y^3}{2}+11Y^6+\cdots\right). \tag{A3}$$

Thus, the positive values of Y specify the separatrix while the negative ones give rise to the lower boundary for vortex-like trajectories. Summarizing all the arguments, we plot the phase portrait of system (26) in Fig. 3.

APPENDIX B: ASYMPTOTIC ANALYSIS OF THE LLD MODEL AS $U \to 0$

In the limit $U \to 0$, we seek an asymptotic solution in the form

$$z=z_0+Uz_1+\cdots. \tag{B1}$$

Substituting the expansion (B1) into Eq. (14), we have

$$(z_0''+z_0^{-3})'=0, \quad z_0''(\infty)=1, \quad z_0(-\infty)=1,$$
$$z_0'(-\infty)=0, \tag{B2}$$
$$(z_1''-3z_0^{-4}z_1)'=(z_0-1)z_0^{-3}, \quad z_1''(\infty)=0,$$
$$z_1(-\infty)=0, \quad z_1'(-\infty)=0. \tag{B3}$$

Integrating (B2), we get

$$z_0''+z_0^{-3}=1. \tag{B4}$$

Considering the solution in the form $z_0'=y(z_0)$, we have $yy'=1-z_0^{-3}$. Integrating the latter accounting for the boundary condition at minus infinity, one obtains

$$y^2=z_0^{-2}+2z_0-3. \tag{B5}$$

One more integration gives

$$x=\sqrt{1+2z_0}+\frac{1}{\sqrt{3}}\ln\frac{\sqrt{1+2z_0}-\sqrt{3}}{\sqrt{1+2z_0}+\sqrt{3}}. \tag{B6}$$

In order to find the first-order term in asymptotic expansion (B1), we integrate (B3) to get

$$z_1''-3z_0^{-4}z_1=\int (z_0-1)z_0^{-3}\,dX. \tag{B7}$$

Taking as a new variable $t=z_0(x)$ $(1<t<\infty)$, we have from (B7)

$$y(t)(y(t)z_1')'-3\frac{z_1}{t^4}=f_1(t), \tag{B8}$$

where

$$f_1(t)=\int \frac{t-1}{t^3}\frac{dt}{y(t)}=-\frac{\sqrt{1+2t}}{t}-\ln\frac{\sqrt{1+2t}-1}{\sqrt{1+2t}+1}. \tag{B9}$$

Seeking the solution to (B8) in the form $z_1=C(t)y(t)$, (B8) is represented as

$$(y^3C')'=f_1. \tag{B10}$$

The first integration of (B10) gives

$$C'=\left(\frac{t}{(t-1)\sqrt{1+2t}}\right)^3 g(t),$$
$$g(t)=-\sqrt{1+2t}-(1+t)\ln\frac{\sqrt{1+2t}-1}{\sqrt{1+2t}+1}+k, \tag{B11}$$

where constant k is dictated by the boundary condition $g(1)=0$

$$k=\sqrt{3}+2\ln\frac{\sqrt{3}-1}{\sqrt{3}+1}=-0.901.$$

In order to calculate $F(U)$ we need only the asymptotic solution z_0 and z_1 as $X \to \infty$ (or $t \to \infty$). Then (B11) gives $z_1 = -k + O(t^{-1/2})$. Substituting in Eq. (12) the asymptotic values of z_0 and z_1 as $X \to \infty$, we obtain

$$F = -3 + 2Uk + O(U^2).$$

[1] E. B. Dussan, "Spreading of liquids on solid-surfaces—Static and dynamic contact lines," Annu. Rev. Fluid Mech. **11**, 371 (1979).
[2] P. G. DeGennes, "Wetting—Statics and dynamics," Rev. Mod. Phys. **57**, 827 (1985).
[3] L. W. Schwartz, H. M. Princen, and A. D. Kiss, "On the motion of bubbles in capillary tubes," J. Fluid Mech. **172**, 259 (1986).
[4] G. F. Teletzke, H. T. Davis, and L. E. Scriven, "How liquids spread on solids," Chem. Eng. Commun. **55**, 41 (1987).
[5] G. F. Teletzke, H. T. Davis, and L. E. Scriven, "Wetting hydrodynamics," Rev. Phys. Appl. **23**, 989 (1988).
[6] A. M. Cazabat, "How does a droplet spread," Contemp. Phys. **28**, 347 (1987).
[7] E. L. Decker, B. Frank, Y. Suo, and S. Garoff, "Physics of contact angle measurement," Colloids Surf., A **156**, 177 (1999).
[8] K. G. Kornev, A. V. Neimark, and A. N. Rozhkov, "Foam in porous media: Thermodynamic and hydrodynamic peculiarities," Adv. Colloid Interface Sci. **82**, 127 (1999).
[9] L. M. Pismen, "Mesoscopic hydrodynamics of contact line motion," Colloids Surf., A **206**, 11 (2002).
[10] F. P. Bretherton, "The motion of long bubbles in tubes," J. Fluid Mech. **10**, 166 (1961).
[11] G. E. P. Elliott and A. C. Riddiford, "Dynamic contact angles and rates of adsorption," Nature (London) **195**, 795 (1962).
[12] G. E. P. Elliott and A. C. Riddiford, "Dynamic contact angles. I. Effect of impressed motion," J. Colloid Interface Sci. **23**, 389 (1967).
[13] A. M. Schwartz and S. B. Tejada, "Studies of dynamic contact angles on solids," J. Colloid Interface Sci. **38**, 359 (1972).
[14] G. Giannotta, M. Morra, E. Occhiello, F. Garbassi, L. Nicolais, and A. Damore, "Dynamic wetting of carbon-fibers by viscous fluids," J. Colloid Interface Sci. **148**, 571 (1992).
[15] R. V. Sedev, C. J. Budziak, J. G. Petrov, and A. W. Neumann, "Dynamic contact angles at low velocities," J. Colloid Interface Sci. **159**, 392 (1993).
[16] D. Y. Kwok, C. J. Budziak, and A. W. Neumann, "Measurements of static and low-rate dynamic contact angles by means of an automated capillary rise technique," J. Colloid Interface Sci. **173**, 143 (1995).
[17] After our article was submitted to Phys. Fluids, there appeared a very interesting paper by Hirasaki and Yang where the authors employ a similar approach to explain the behavior of dynamic contact angle at moderate velocities [G. I. Hirasaki and S. Y. Yang, "Dynamic contact line with disjoining pressure, large capillary numbers, large angles and pre-wetted, precursor, or entrained films," in *Contact Angle, Wettability and Adhesion*, edited by K. L. Mittal (VSP, New York, 2002), Vol. 2].
[18] B. V. Derjaguin, "Correct form of the equation of capillary condensation in porous bodies in application to the separation of adsorption and capillary condensation in slits and porous bodies of known structure and determination of their structure by adsorption and sorption isotherms" (reprinted from Proceedings of the 2nd International Congress on Surface Activity, Vol. 2, pp. 153–159, 1957), Prog. Surf. Sci. **40**, 126 (1992).
[19] B. V. Derjaguin, N. V. Churaev, and V. M. Muller, *Surface Forces* (Plenum, New York, 1987).
[20] C. J. Van Oss, *Interfacial Forces in Aqueous Media* (Marcel Dekker, New York, 1994).
[21] K. G. Kornev, I. K. Shingareva, and A. V. Neimark, "Capillary condensation as a morphological transition," Adv. Colloid Interface Sci. **96**, 143 (2002).
[22] B. V. Derjaguin and N. V. Churaev, *Wetting Films* (Nauka, Moscow, 1984).
[23] V. M. Starov, "Equilibrium and hysteresis contact angles," Adv. Colloid Interface Sci. **39**, 147 (1992).
[24] L. H. Tanner, "Spreading of silicone oil drops on horizontal surfaces," J. Phys. D **12**, 1473 (1979).
[25] A. Hamraoui, K. Thuresson, T. Nylander, and V. Yaminsky, "Can a dynamic contact angle be understood in terms of a friction coefficient?" J. Colloid Interface Sci. **226**, 199 (2000).
[26] S. Kalliadasis and H. C. Chang, "Apparent dynamic contact-angle of an advancing gas–liquid meniscus," Phys. Fluids **6**, 12 (1994).
[27] R. Lucas, "Ueber das zeitgesetz des kapillaren aufstiegs von flussigkeiten," Kolloid-Z. **23**, 15 (1918).
[28] E. W. Washburn, "The dynamics of capillary flow," Phys. Rev. **17**, 273 (1921).
[29] O. V. Voinov, "Asymptotics of the viscous-liquid free-surface at the creeping motion and the dependence of wetting angle on the velocity," Dokl. Akad. Nauk SSSR **243**, 1422 (1978).
[30] L. D. Landau and V. G. Levich, "Dragging of a liquid by a moving plate," Acta Physicochim. URSS **17**, 42 (1942).
[31] B. V. Derjaguin, "Thickness of the liquid film adhering to a moving thread," Dokl. Akad. Nauk SSSR **39**, 11 (1943).
[32] V. D. Sobolev, N. V. Churaev, M. G. Velarde, and Z. M. Zorin, "Surface tension and dynamic contact angle of water in thin quartz capillaries," J. Colloid Interface Sci. **222**, 51 (2000).
[33] A. De Ryck, "The effect of weak inertia on the emptying of a tube," Phys. Fluids **14**, 2102 (2002).
[34] L. M. Pismen, B. Y. Rubinstein, and I. Bazhlekov, "Spreading of a wetting film under the action of van der Waals forces," Phys. Fluids **12**, 480 (2000).
[35] W. F. Ford, C. C. Grosjean, H. Demeyer, W. B. Jordan, A. C. King, A. D. Osborne, and J. E. Wilkins, "A 3rd-order differential-equation," SIAM Rev. **34**, 121 (1992).
[36] B. R. Duffy and S. K. Wilson, "A third-order differential equation arising in thin-film flows and relevant to Tanner's law," Appl. Math. Lett. **10**, 63 (1997).
[37] H. Hervet and P. G. Degennes, "The dynamics of wetting—precursor films in the wetting of dry solids," Comptes Rendus De L Academie Des Sciences Serie Ii **299**, 499 (1984).
[38] K. Kornev and G. Shugai, "Thermodynamic and hydrodynamic peculiarities of a foam lamella confined in a cylindrical pore," Phys. Rev. E **58**, 7606 (1998).
[39] T. E. Mumley, C. J. Radke, and M. C. Williams, "Kinetics of liquid liquid capillary rise. I. Experimental observations," J. Colloid Interface Sci. **109**, 398 (1986).
[40] T. E. Mumley, C. J. Radke, and M. C. Williams, "Kinetics of liquid liquid capillary rise. II. Development and test of theory," J. Colloid Interface Sci. **109**, 413 (1986).
[41] M. Y. Zhou and P. Sheng, "Dynamics of immiscible-fluid displacement in a capillary tube," Phys. Rev. Lett. **64**, 882 (1990).
[42] J. P. Stokes, M. J. Higgins, A. P. Kushnick, S. Bhattacharya, and M. O. Robbins, "Harmonic generation as a probe of dissipation at a moving contact line," Phys. Rev. Lett. **65**, 1885 (1990).
[43] S. Ping and M. Y. Zhou, "Immiscible-fluid displacement—Contact-line dynamics and the velocity-dependent capillary pressure," Phys. Rev. A **45**, 5694 (1992).